Journal of Environmental Management 151 (2015) 76–86

Contents lists available at ScienceDirect

Journal of Environmental Management

journal homepage: www.elsevier.com/locate/jenvman

Combined impacts of future climate and land use changes on discharge, nitrogen and phosphorus loads for a Canadian river basin

A. El-Khoury [a], O. Seidou [a, *], D.R. Lapen [b], Z. Que [a], M. Mohammadian [a], M. Sunohara [b], D. Bahram [b]

[a] Department of Civil Engineering, University of Ottawa, 161 Louis Pasteur, Ottawa, ON, K1N 6N5, Canada
[b] Agriculture and Agri-Food Canada, 960 Carling Ave, Ottawa, ON, K1A 0C6, Canada

ARTICLE INFO

Article history:
Received 22 September 2013
Received in revised form
20 November 2014
Accepted 4 December 2014
Available online 20 December 2014

Keywords:
Land use projections
Climate change
Nitrogen
Phosphorus
SWAT

ABSTRACT

Both climate and land use changes can influence water quality and quantity in different ways. Thus, for predicting future water quality and quantity trends, simulations should ideally account for both projected climate and land use changes. In this paper, land use projections and climate change scenarios were integrated with a hydrological model to estimate the relative impact of climate and land use projections on a suite of water quality and quantity endpoints for a Canadian watershed. Climatic time series representing SRES change scenario A2 were generated by downscaling the outputs of the Canadian Regional Climate Model (version 4.1.1) using a combination of quantile–quantile transformation and nearest neighbor search. The SWAT (Soil and Water Assessment Tool) model was used to simulate streamflow, nitrogen and phosphorus loading under different climate and land use scenarios. Results showed that a) climate change will drive up maximum monthly streamflow, nitrate loads, and organic phosphorus loads, while decreasing organic nitrogen and nitrite loads; and b) land use changes were found to drive the same water quality/quantity variables in the same direction as climate change, except for organic nitrogen loads, for which the effects of the two stressors had a reverse impact on loading.

1. Introduction

Studies that address the combined effects of climate change and land use changes in tandem on water quantity and/or quality have been documented variably in literature (Liu et al., 2000; Barlage et al., 2002; Legesse et al., 2003; Tu, 2009; Wilson and Weng, 2011; Dunn et al., 2012; Felzer, 2012; Sample et al., 2012; Tong et al., 2012; Seung-Hwan et al., 2013; Kim et al., 2013). Each of these studies involves numerical experiments whereby a calibrated hydrological model is forced with climatic inputs representing one or several global warming scenarios, and using current and/or projected land use maps.

Differences in these studies lie in the location of the study area, the hydrological model, the type of water quantity and quality variable under scrutiny, and the way climate change and land use scenarios are generated. Hydrological models range from very simple water balance models (Liu et al., 2000; Sample et al., 2012) to sophisticated watershed models, such as the Annualized Agricultural Non-Point Source model (AnnAGNPS: Bingner et al., 2007) and the Soil Water Assessment Tool (SWAT: Wilson and Weng, 2011; Kim et al., 2013) which are capable of simulating loads and concentrations of a variety of water quality targets. The approaches used to evaluate climate change vary as well: Liu et al. (2000), Legesse et al. (2003), and Tong et al. (2012) utilized the Delta-change method which consist of adding arbitrarily chosen variations to historical data sets to represent global warming. Others used the outputs of global and regional climate models without any processing (Tu, 2009; Kim et al., 2013), or in combination with a statistical downscaling approach such as the Delta-change method (e.g. Dunn et al., 2012; Sample et al., 2012; Tong et al., 2012), bias correction (Wilson and Weng, 2011; Felzer, 2012), weather generators (Dunn et al., 2012; Seung-Hwan et al., 2013), or regression-based downscaling (e.g. Seung-Hwan et al., 2013).

However, Delta-change downscaling method and bias-corrected global climate model output generation may be too simplistic to characterize climate trends. Raw global climate outputs suffer from distortion even after bias removal, and the Delta-change method is often unable to capture changes in climate variability important for

* Corresponding author.
E-mail address: oseidou@uottawa.ca (O. Seidou).

http://dx.doi.org/10.1016/j.jenvman.2014.12.012

use as input to regional hydrological simulations. Dibike and Coulibaly (2005), Chiew et al. (2010) and Chen et al. (2012) for instance, have shown that streamflow simulated by forcing hydrological models using climate data obtained using different downscaling techniques can vary or even give conflicting trends. Burger et al. (2012, 2013) have shown that downscaling techniques have very unequal performance in reproducing climate extremes. Burger et al. (2013) showed that downscaled climate extremes were more sensitive to the choice of the downscaling technique than the emission scenario, the climate model, and the geographic location. Given that extreme climatic events are linked to variability and climate variable distributions, and that hydrological processes can be very sensitive to extreme events, consequently the choice of downscaling technique is crucial for representing more realistic future hydrological scenarios.

Land use projection methods used in the above papers range from generalized assumptions about future conversions (e.g. Legesse et al., 2003; Tu, 2009; Dunn et al., 2012; Sample et al., 2012) to detailed land use allocation modeling platforms based on geographic and socio-economic drivers (e.g. Kim et al., 2013; Seung-Hwan et al., 2013). The choice of the land use model and its ability to produce realistic projections will impact modeling outputs in a potentially profound way in many situations where land use conversions play a significant role in watercourse impairment. Such situations are not uncommon as recent studies even suggest that the consequences of future land use changes on the water cycle may outweigh those from associated with climate change (e.g. Sala, 2000).

The objective of this study was to estimate the tandem impacts of climate change and land use changes on streamflow and nitrogen and phosphorus loads for a Canadian river basin under mixed, but predominately agricultural, land use activities (Fig. 1). Hydrological simulations were run using the SWAT eco-hydrological model, for a variety of future climatic and land use configurations. The climatic data sets and the land use configuration sets contained both present and future (predicted) conditions. The impact of global warming (climate scenarios) and land use change scenarios on prediction endpoints, was analyzed to characterize the relative importance of these drivers on future changes of the hydrological regime. From a local water resources manager or stakeholder perspective, results from this study could support watershed stewardship initiatives within a climate and land use change adaptation perspective. For example, findings from studies such as this could be used to help: sustain protection of natural habitat (eg., wooded areas and wetlands), define plans for long term land use zoning that is protective of water quality, and define long term impacts on ecological targets, such as algal growth, in surface water systems.

The current study differs from previous works dealing with the combined impacts of climate and land use changes on hydrological variables in the following ways:

1. The number and nature of water quality and quantity variables assessed.
2. The projected land use changes were generated with a detailed land use projection model that has been successfully modified and validated for the study area (El-Khoury et al., 2014). The model projected a large increase in cropland areas (from 62% in 2011 to 76% in 2050) and urban areas (0.2% in 2011 to 1% in 2050) and a decrease in forested areas (from 33% in 2011 to 19% in 2050). It also projected a relatively rapid urbanization in the areas close to the Ottawa/Gatineau metropolitan area and the disappearance of small forested areas and their replacement with croplands throughout the watershed.

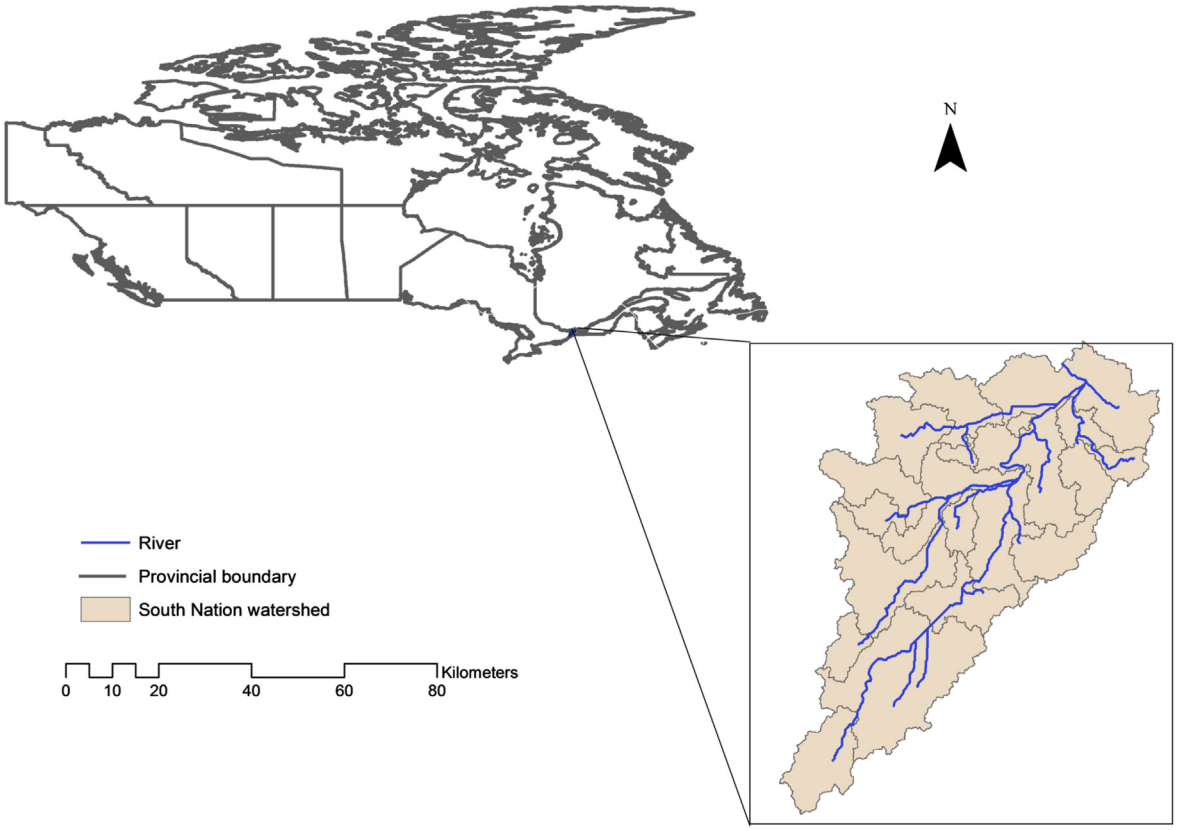

Fig. 1. Location of the South Nation watershed in Ontario, Canada.

3. The climate change scenarios were derived from the outputs of a Regional Climate Model (RCM), and downscaled with techniques that allow for a change in precipitation and temperature variability in the future. This is an improvement over the Delta-change method which does not allow for a change of variability in the future. It also provides more realistic data sets than downscaling techniques such as those implemented in SDSM (Semenov and Barrow, 2002) and LARS-WG (Wilby et al., 2002). SDSM and LARS-WG are typically used by independently downscaling the data at each climate station in the study area. As a result, the inter-station correlation structure is lost after the downscaling. Given that hydrological extremes are caused by wet or dry conditions recorded at most stations in the model, using LARS-WG or SDSM would potentially lead to an underestimation of the frequency of extreme events. The outputs of the proposed downscaling method will inherit the spatial and temporal correlation structure of the RCM outputs, and therefore is more realistic than the results of downscaling techniques applied on a station by station or variable by variable basis.

2. Methods and materials

2.1. The SWAT model

The SWAT model (Arnold et al., 1998) is a process-based hydrology and water quality model, designed to estimate impacts of land management practices on water quantity and quality in complex watersheds. It consists of eight major components: agricultural management, crop growth, hydrology, nutrients, pesticides, sedimentation, soil temperature, and weather. It is a semi-distributed physically-based and computationally efficient model developed for long-term continuous simulations. The setup of the SWAT model and its calibration are described in the next subsections.

2.1.1. Model setup

1. Hydrometeorological Data: Daily (1971–2008) precipitation (PCP), maximum temperature (TMAX), minimum temperature (TMIN), and wind speed (WND) data were acquired from the online database of the National Climate Data and Information Archive (Environment Canada, 2008). Net solar radiation (SLR) and relative humidity (HMD) time series were extracted from the National Centers for Environmental Prediction/National Center for Atmospheric Research (NCEP/NCAR) reanalysis archive (Kalnay et al., 1996). Maximum temperature, minimum temperature, precipitation and wind speed were interpolated over the delineated subwatersheds using the Thiessen Polygon method. Given that a climate variable may not be available on a given day in the study period, the number of stations involved in the interpollation is different for each day. Only the closest NCEP/NCAR reanalysis grid point was used given that the watershed is small compared to the spatial resolution of the NCEP/NCAR reanalysis grid. The 1971–2008 measured streamflow, total N, total P, and sediment loads were obtained from the Provincial Water Quality Monitoring Network (Ministry of the Environment, 2009). These observed water quantity and quality data were used for model calibration and validation.
2. Digital Elevation Model: a 90 m Digital Elevation Data (DEM) was downloaded from the United States Geological Survey website. It was derived from the fourth version of Shuttle Radar Topography Mission (SRTM) data set, which is a global coverage full resolution digital elevation in which gaps were filled (Reuter et al., 2007). The DEM was used to delineate the watershed boundary, along with 18 subwatersheds as presented on Figure 1.
3. Land use and Soil coverages: Soil parameters such as hydrologic soil group, soil layer, soil texture, saturated hydraulic conductivity, and organic matter were derived from the Soil Landscapes of Canada version 3.2 (Soil Landscapes of Canada Working Group, 2010). Seven soil layers covering 0–1.3 m depth (20 cm depth for the six first layers; 10 cm for the last one) were defined and the properties of each layer were set to the average properties calculated from the SLC records. Spatial and temporal land use data were obtained from the Eastern Ontario Water Resources Management Study (CH2MHILL, 2001). A total of six main land use classes were defined: cropland, forage land, forest, bare, urban, water, other (undefined land uses).
4. Dam operation: There are two dams (the Chesterville dam and the Crysler Dam) as well as five water control weirs on the rivers. Only the Chesterville dam is operated by the conservation authorities to keep water level at a certain level without specific periods of filling or emptying; the hydraulic structures on the rivers are therefore not expected to affect monthly flows; they were therefore not included in the SWAT model.
5. *Sub-watersheds and Hydrological Response Units*: At the end of the process, a model with 18 subwatersheds was obtained (Fig. 2). A total of 1067 hydrological response units (HRUs) were obtained, 721 being agricultural HRUs. Crop rotations in the HRUs were set following Que (2011). The characteristics of the South Nation (SN) SWAT model are summarized in Table 1.

2.1.2. Calibration and validation

The calibration process was conducted using the SWAT-CUP program (Abbaspour et al., 2007) using the SUFI2 (Sequential Uncertainty Fitting) algorithm, and involved a total of 26 SWAT parameters that are listed in Table 2. Six water quantity and quality variables were considered: streamflow (FLOW), nitrate-nitrogen (NO_3–N), nitrite-nitrogen (NO_2–N), organic nitrogen (OrgN), organic phosphorus (OrgP), and mineral phosphorus (MinP). The objective function was the Nash-Suttcliffe coefficient at the oulet of the watershed. The calibration and validation period for each of the output parameters are presented in Table 3.

2.2. Downscaling/bias correction of the Canadian RCM outputs

The 1950–2011 gridded precipitation, wind speed, maximum and minimum temperature data sets simulated over Eastern Canada using the Canadian RCM under SRES scenario A2 were downloaded from the Environment Canada Data Access Interface (Gachon et al., 2009). The time series of each variable was extracted for each of the 18 subwatersheds in the SWAT simulation framework. Given that the accuracy of simulated streamflow and water quality parameters is very sensitive to the statistical distribution of the climate variable, a quantile–quantile transformation was applied to the three extracted climate variables (precipitation, minimum and maximum temperature). A nearest-neighbor approach (described later in the section) was used to estimate the two remaining variables (relative humidity and solar radiation). Both the quantile–quantile transformation and nearest-neighbor search were conducted on a monthly basis.

2.2.1. Quantile–quantile transformation of RCMs precipitation, wind speed and temperature

The quantile–quantile transformation (Jakob Themeßl et al., 2011; Maraun et al., 2010), also called quantile mapping or quantile matching, aims to make the statistical distribution of a given climate variable as close as possible to the statistical distribution of

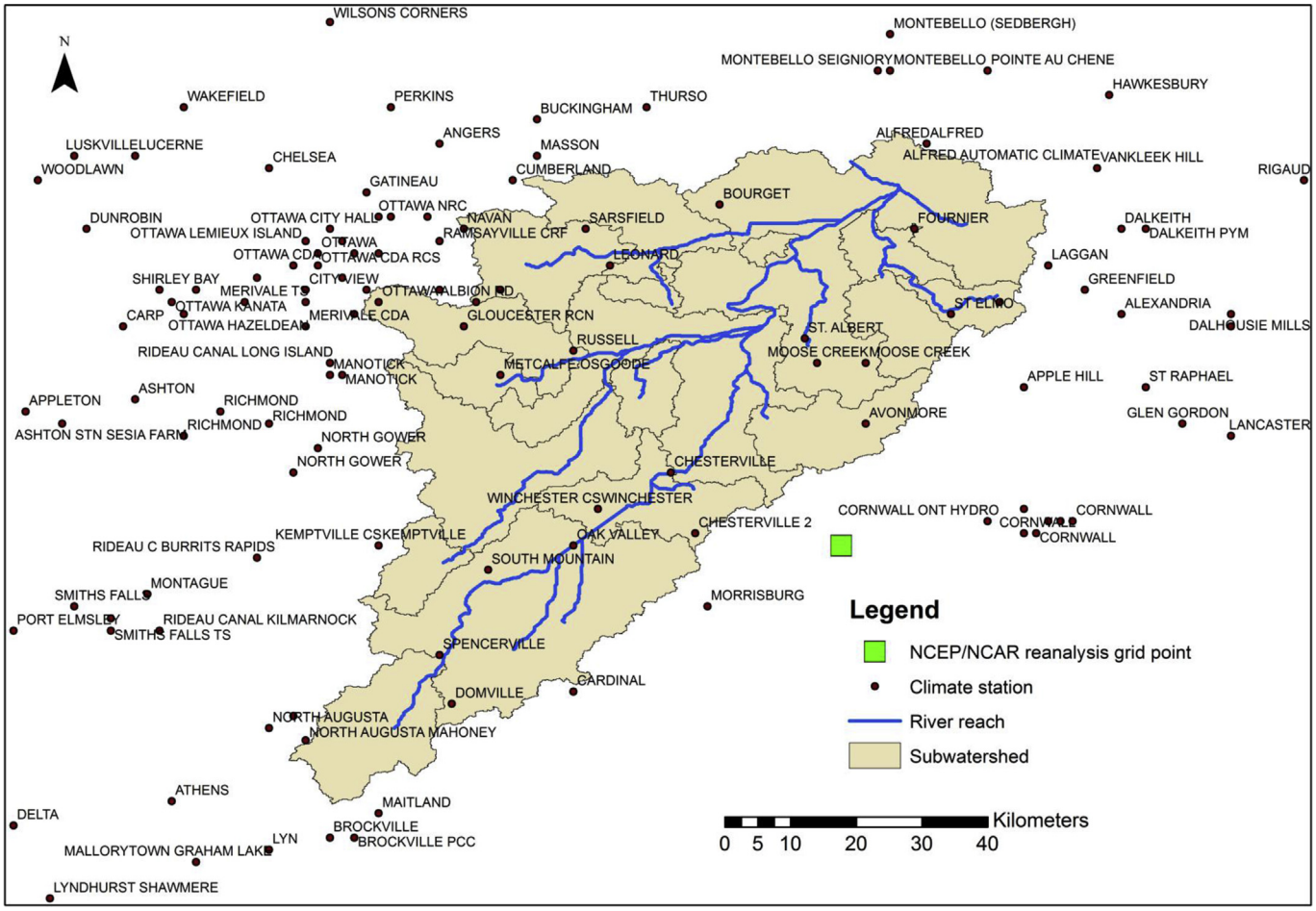

Fig. 2. Delineated sub-watersheds, river reaches, climate stations and NCEP/NCAR reanalysis grid points.

the observed variable in the historical period in question. The transformation for a given month and a given variable is performed as follows:

1. The historical data is split into a calibration period (1971–1980) and a validation period (1981–2010). The daily time series of the month are extracted for both periods from both observations and RCM simulations
2. An empirical cumulative distribution function is developed using the observations on the calibration period. Another cumulative distribution function is developed using the RCM outputs on the calibration period
3. Corrected RCM simulations are generated on the validation period and future periods using the following transformation
4. For all variables except precipitation, empirical probability distribution functions (PDF) of the observed, RCM-simulated and corrected variable are plotted. The PDFs are then visually compared on both the calibration and validation periods. The probability mass function (PMF) of precipitation occurrence (defined as intensity >1 mm/day) as well as the PDF of precipitation intensity on rainy days are generated. If the PDF (or PMF) of the corrected variable is closer to the PDF of the observations than the PDF (or PMF) of the non-corrected variable, the quantile–quantile transformation is applied to future RCM simulations of that particular variable.

Table 1
South Nation River SWAT model characteristics.

Watershed area	3858 km^2
Number of sub-watersheds	18
Number of HRUs	1067
Length of climate time series	1971–2008
Percentage of cropland area	57.81%
Percentage of forested area	41.03%

As explained at the end of the introduction, one advantage of the above downscaling method is that the downscaled data sets display a similar spatial and temporal correlation structure as the RCM outputs. For example, if a high precipitation amount is simulated at one station, it is probable that all surrounding stations will have a high value of precipitation. Several existing downscaling models such as LARS-WG (Semenov and Barrow, 2002) and SDSM (Wilby et al., 2002) work on a station by station basis and fail to reproduce that temporal and spatial coherence structure. It is well known that simulations of extreme flow by a rainfall-runoff model for instance, are directly linked to that temporal correlation: extreme floods are usually due to large precipitation events recorded at most stations used in the model. Given that the SWAT model of the river basin contains several climate stations, using LARS-WG or SDSM would lead to an unrealistic simulation of the frequency of extreme events.

2.2.2. Nearest-neighbor search for relative humidity, net solar radiation and wind speed

Future estimates of relative humidity and net solar radiation were generated using a nearest-neighbor approach: for each day d in the future period, a day d_1 from the same month is selected

Table 2
Parameters used for calibration and validation.

No	Variation	Parameter	Definition	Fitted value
1	Absolute	CANMX	Maximum canopy storage (mm)	216.25
2	Relative	CN2	SCS curve number (condition II)	0.28
3	Absolute	DEP_IMP	Depth to the impervious layer (mm)	1300.00
4	Relative	OV_N	Manning coefficient for overland flow	−1.00
5	Absolute	GW_DELAY	Groundwater delay (days)	30.00
6	Relative	SOL_AWC	Soil layer available water content (mm)	1.63
7	Relative	SOL_K	Soil hydraulic conductivity (cm/h)	−0.50
8	Relative	HRU_SLP	HRU slope	0.27
9	Absolute	CH_K2	Muskingum routing coefficient	1500.00
10	Relative	CH_W2	Channel width coefficient	9.00
11	Relative	NPERCO	N percolation coefficient	−0.75
12	Absolute	SMFMX	Maximum snowmelt rate coefficient	18.80
13	Absolute	SMFMN	Minimum snowmelt rate coefficient	1.80
14	Absolute	ESCO	Soil evaporation compensation coefficient	0.90
15	Absolute	USLE_K	Universal Soil Loss Equation coefficient	0.10
16	Absolute	USLE_P	Universal Soil Loss Equation coefficient	1.00
17	Absolute	ERORGN	Organic N enrichment ratio	0.02
18	Absolute	ERORGP	Organic P enrichment ratio	0.00
19	Absolute	BC1	Rate constant for the oxidation of ammonia at 20° C (1/day)	4.15
20	Absolute	BC2	Rate constant for the oxidation of nitrite to nitrate at 20° C (1/day)	1.50
21	Absolute	BC3	Local rate constant for hydrolysis of organic nitrogen to NH_4^+ at 20° C (1/day)	0.01
22	Absolute	BC4	Local rate constant for phosphorus mineralization at 20° C (1/day)	0.34
23	Relative	PHOSKD	Phosphorus soil partitioning coefficient (m^3/Mg)	5.00
24	Absolute	PPERCO	P percolation coefficient	500.00
25	Absolute	DIS_STREAM	Average distance to streams (km)	31.50

from the historical period so that the absolute difference between the average temperature of day d and the average temperature of day d_1 is minimum. The measured solar radiation and relative humidity of day d_1 is assigned to day d.

At the end of the process, future values of all the six climate variables (precipitation, minimum and maximum temperature, wind speed, relative humidity and solar radiation) required to run a SWAT model were generated for each of the 18 subwatersheds.

2.3. Numerical experiments

The following experiments were performed in order to assess how the six selected water quality/quantity targets responded to changes in climate and land use:

Experiment 1: Simulation using observed 2005 land use and observed 1985–2010 climate data

Experiment 2: Simulation using the observed 2005 land use and the projected 2025–2050 climate change data

Experiment 3: Simulation using the observed 1985–2010 climate data, and 2025–2050 land use projection data. Since both the climate and land use are changing in this scenario, the climate of year $(1984 + i)$ is simulated with the land use of year $(2024 + i)$ where i varies from 1 to 26.

Experiment 4: Simulation using the projected 2025–2050 land use and the projected 2025–2050 climate change data

The impacts of climate change alone can be estimated by comparing the simulated water quantity and quality parameters of experiments 1 and 2; the impacts of land use change can be estimated by comparing experiments 1 and 3; finally, the combined impacts of climate change and land use changes can be estimated by comparing experiments 1 and 4. Average monthly loads as well as boxplots of the monthly and annual load of each parameter were generated.

3. Results and discussion

3.1. Hydrological model calibration and validation

Observed and simulated time series of the selected parameters are presented in Fig. 3 (Q, NO_2–N and NO_3–N) and Fig. 4 (OrgN, OrgP and MinP). The calibration and validation performance indices are listed in Table 3. The calibration Nash Suttcliffe coefficient ranged from 0.73 for streamflow to 0.24 for nitrite, while the coefficient of determination ranged from 0.78 for streamflow to 0.35 for nitrite and organic phosphorus. The validation Nash Sutcliffe coefficients ranged from 0.44 to 0.68, except for nitrite, where it is negative. The low values for nitrite were expected given that it is known to be a very transient chemical (Philips et al., 2002). The routines implemented in SWAT will likely capture only a few of the processes affecting the nitrite balance. The overall performance of the model with respect to six different water quality and quantity parameters suggest that the model reasonably captured the most important hydrological processes in the basin. It can therefore be used with a reasonable degree of confidence in the planned numerical experiments.

Table 3
SWAT calibration and validation result for each hydrological and water quality parameter.

Variable	Period	Nash	R^2
Streamflow (m^3 s^{-1})	Calibration (1973/1–1994/6)	0.73	0.78
	Validation (1994/7–2008/12)	0.68	0.7
Nitrate-nitrogen (kg N $month^{-1}$)	Calibration (1988/1–1995/11)	0.53	0.57
	Validation (1996/5–2001/10)	0.56	0.61
Nitrite-nitrogen (kg N $month^{-1}$)	Calibration (1987/10–1996/6)	0.24	0.35
	Validation (1996/7–2001/9)	−0.13	0.83
Organic Nitrogen (kg N $month^{-1}$)	Calibration (1987/10–1996/6)	0.52	0.59
	Validation (1996/7–2001/9)	0.65	0.77
Organic Phosphorus (kg P $month^{-1}$)	Calibration (1973/1–1996/1)	0.28	0.35
	Validation (1996/2–2001/9)	0.44	0.54
Mineral Phosphorus (kg P $month^{-1}$)	Calibration (1973/1–1996/1)	0.25	0.42
	Validation (1996/2–2001/9)	0.63	0.64

3.2. Downscaling results

The application of the quantile–quantile transformation significantly improved the distribution of RCM precipitation, wind and air temperature. A few examples of improved distributions are presented in Fig. 5 (probability of precipitation >1 mm/day on subwatershed 1), Fig. 6 (wet day precipitation intensity) and Fig. 7 (minimum air temperature distribution on subwatershed 1). In each of these figures, the Probability Density Function (PDF) or the Probability Mass Function (PMF) of the climate variable is plotted for each month for both the calibration and validation periods. It can be visually assessed that the distribution of the corrected RCM data is almost identical to the distribution of the observations for the calibration period; it is always closer to the distribution of the observations than the distribution of the uncorrected RCM data. For instance, the minimum air temperature in subwatershed 1 was systematically underestimated by the RCM (Fig. 7), but the quantile–quantile transformation scaled it back to the right magnitude. In terms of magnitude, results show an increase of 1.21° of minimum temperature (from 11.37° to 12.58°) and 1.55° in maximum temperatures (from 1.59° to 3.15°) between the 1985–2010 and 2025–2050 periods. Precipitation increased by 3.5% from 992 mm y^{-1} to 1027 mm y^{-1} Wind speeds did not vary significantly between the current and future period (−0.7%).

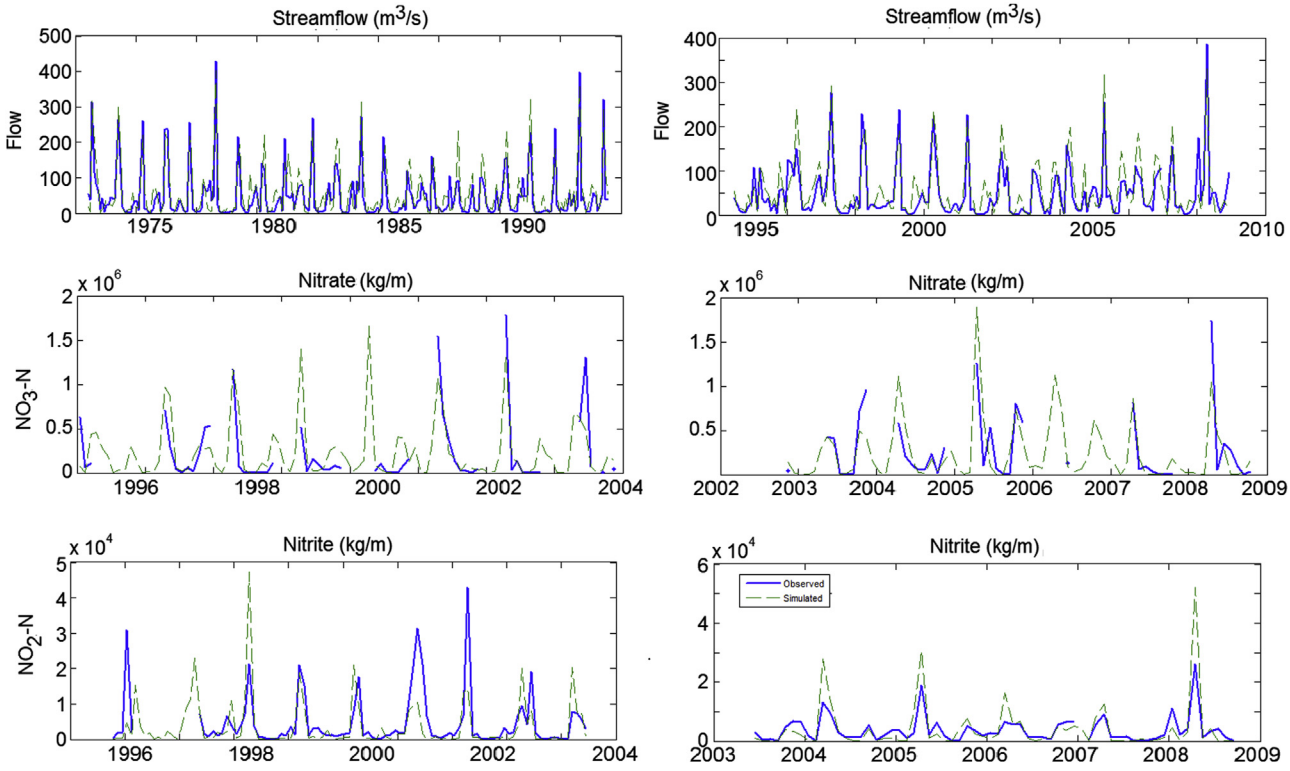

Fig. 3. Simulated (dashed green line) and observed (continuous blue line) time series, streamflow, nitrate (NO_3–N) and nitrite (NO_2–N). (For interpretation of the references to color in this figure legend, the reader is referred to the web version of this article.)

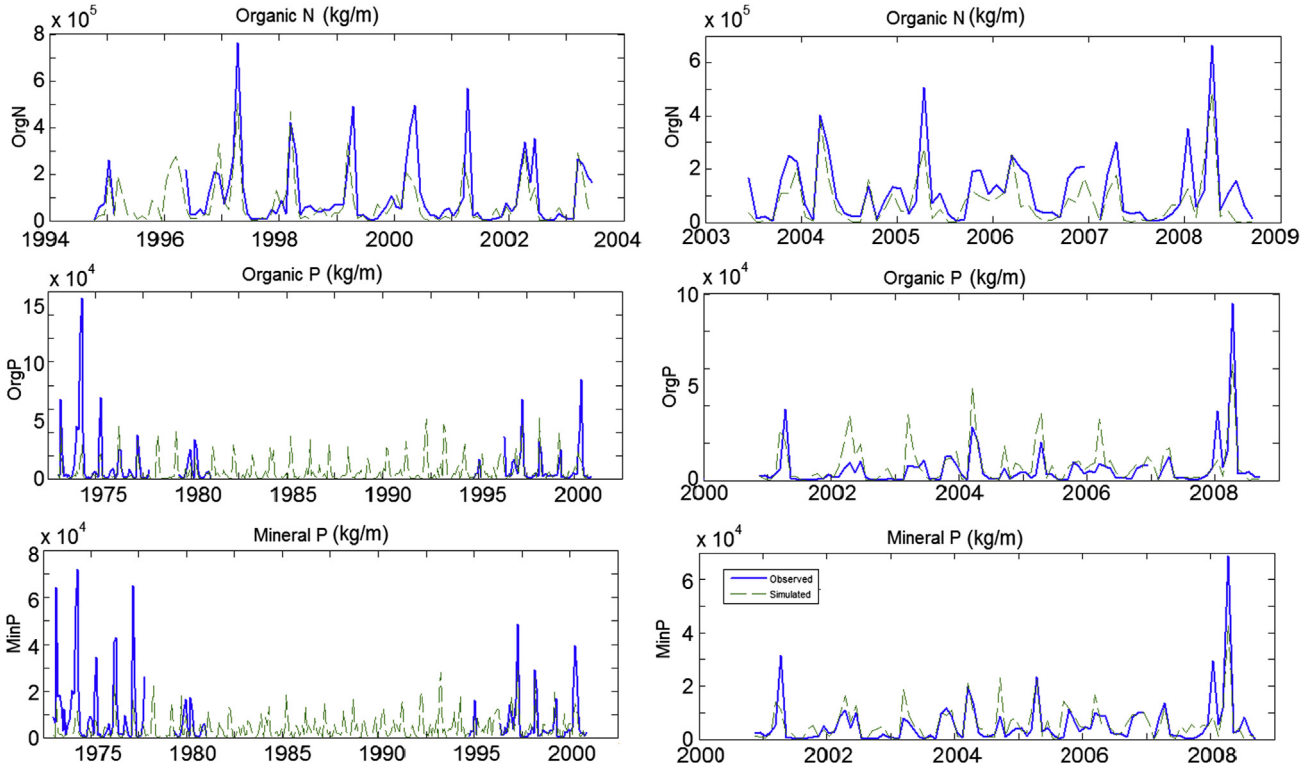

Fig. 4. Simulated (dashed green line) and observed (continuous blue line) time series, organic N, organic P and mineral P. (For interpretation of the references to color in this figure legend, the reader is referred to the web version of this article.)

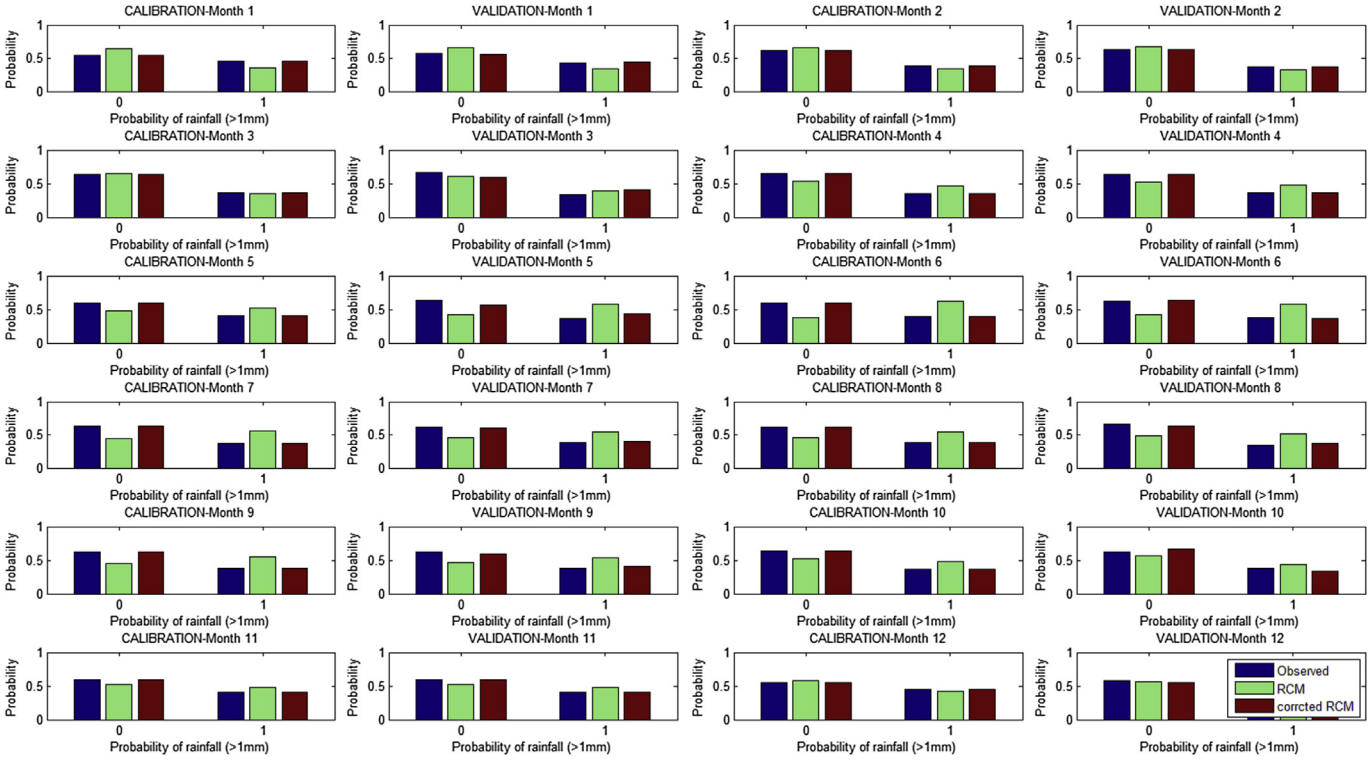

Fig. 5. Empirical PDF of observed (blue bars), RCM-simulated (green bars) and corrected (red bars) precipitation occurrence. (For interpretation of the references to color in this figure legend, the reader is referred to the web version of this article.)

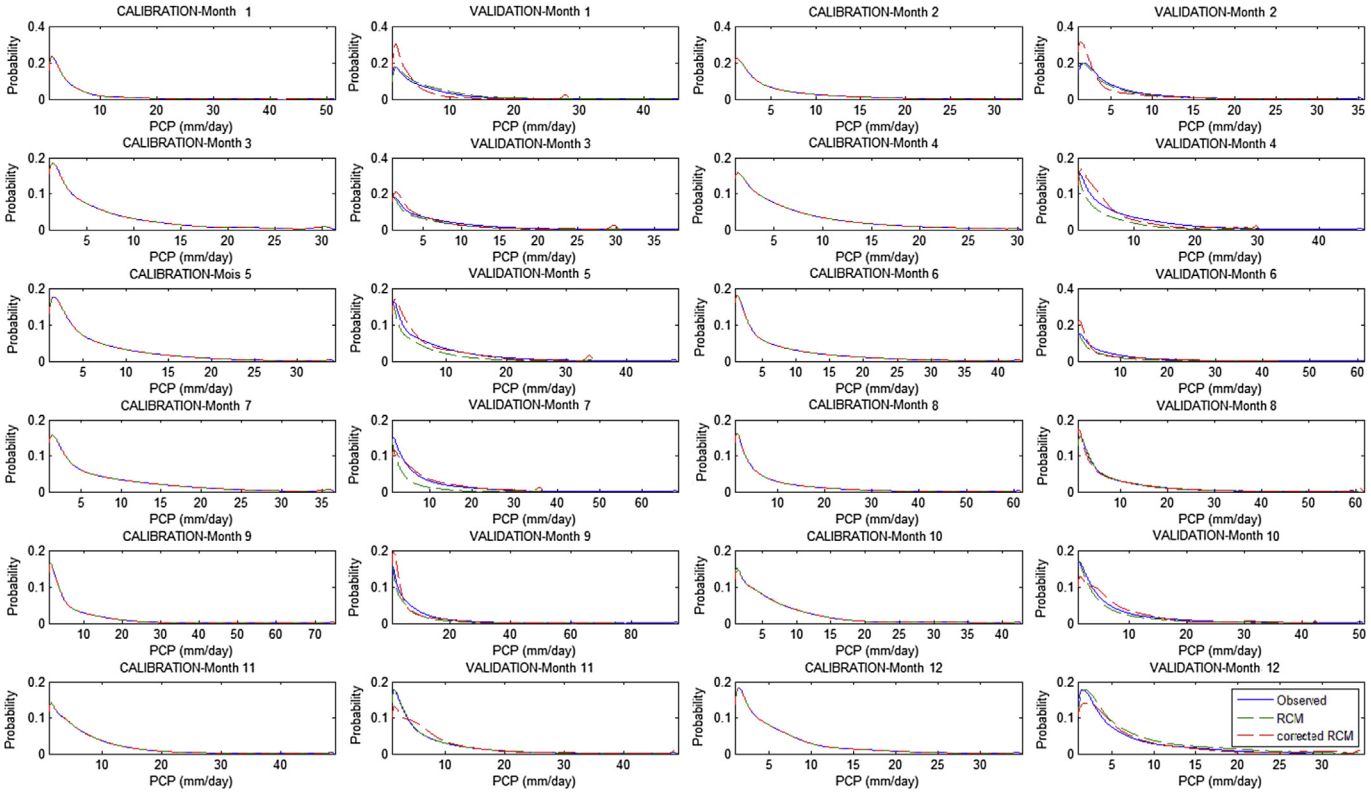

Fig. 6. Empirical PDF of observed (continuous blue line), RCM-simulated (dashed green line) and corrected (dashed red line) precipitation density.

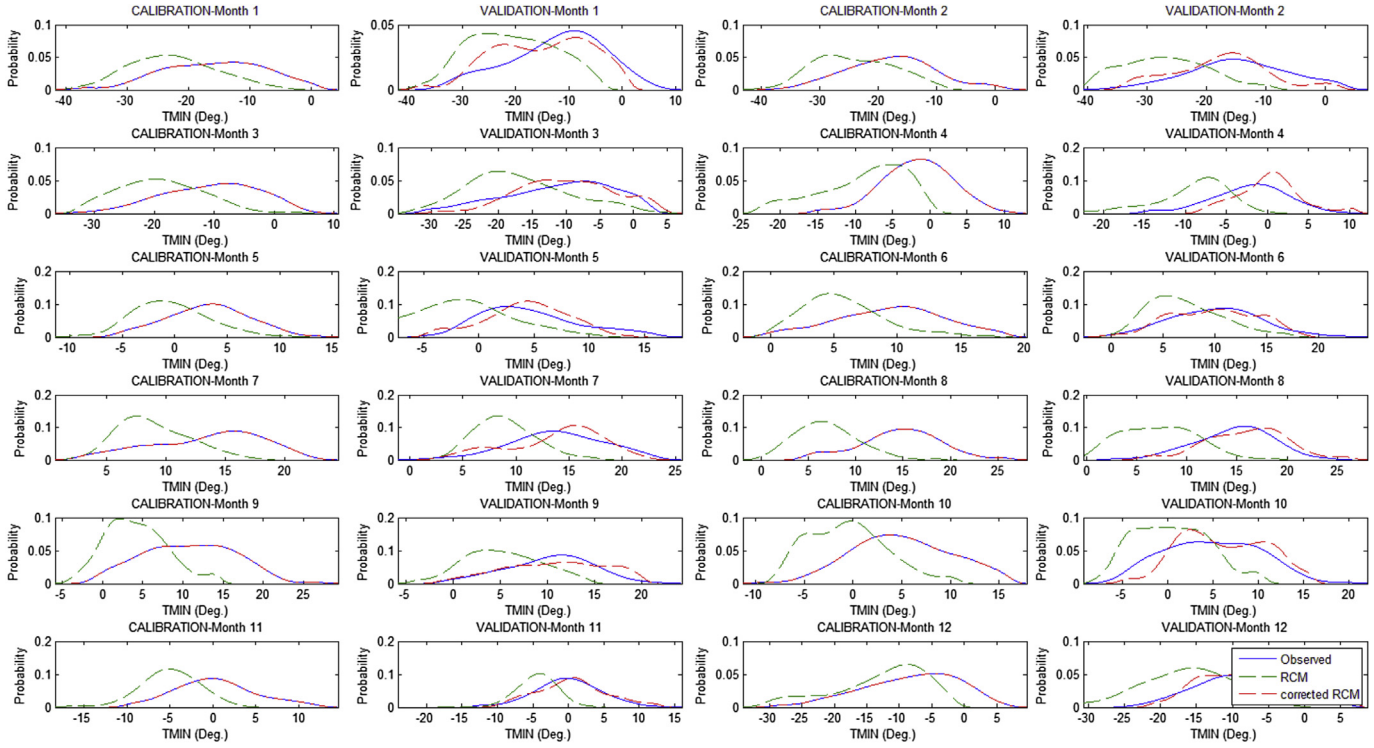

Fig. 7. Empirical PDF of observed (continuous blue line), RCM-simulated (dashed green line) and corrected (dashed red line) minimum temperature on sub-watershed 1.

3.3. *River discharge and P and N loads for different climate/land use scenarios*

Figs. 8–13 show average monthly load (upper panel) and boxplots of the maximum average monthly load (bottom left panel) and the annual load (bottom right panel) for all selected parameters, and for all experiments. The percentages of variation in the annual load and the monthly maximum load of each variable are listed in Table 4. Results show that the average hydrograph of

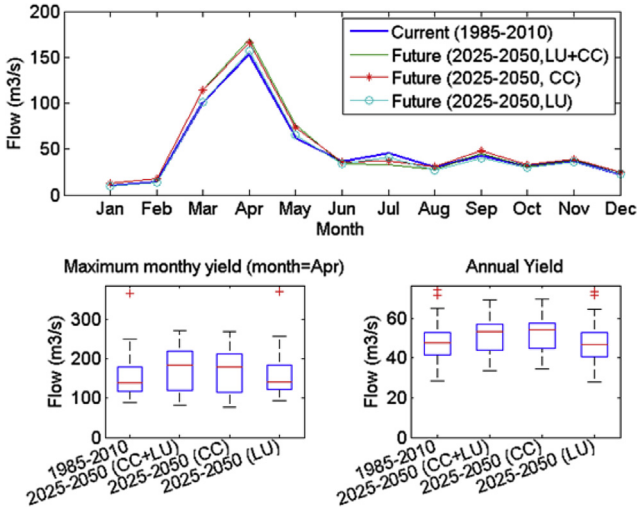

Fig. 8. Climate and land use change impacts on streamflow. Upper panel: average monthly streamflow under current climate and land use (continuous blue line), under future land use and climate (continuous green line), under current land use and future climate (red line with star dots) and under future land use and current climate (cyan line with circular dots); Lower-left panel: boxplot of the maximum monthly load; Lower-right panel: boxplot of the annual load; CC: accounting for climate change; LU: accounting for land use changes. (For interpretation of the references to color in this figure legend, the reader is referred to the web version of this article.)

Table 4
Climate and land use change impacts on water quantity and quality parameters.

Variable	Experiment	Maximum monthly load		Annual load	
		Average	Variation (%)	Average	Variation (%)
Streamflow (m^3/s)	1985–2010	152	–	22	–
	2025–2050 (CC + LU)	169	11.0	25	12.3
	2025–2050 (CC)	165	8.5	24	11.2
	2025–2050 (LU)	156	2.6	22	1.2
Nitrate (kg $month^{-1}$)	1985–2010	202,257	–	64,621	–
	2025–2050 (CC + LU)	226,047	11.7	74,638	15.5
	2025–2050 (CC)	205,238	1.4	64,568	−0.1
	2025–2050 (LU)	223,700	10.6	73,718	14.0
Nitrite (kg $month^{-1}$)	1985–2010	182,938	–	2078	–
	2025–2050 (CC + LU)	147,198	−19.6	2140	2.9
	2025–2050 (CC)	155,465	−15.1	1884	−9.4
	2025–2050 (LU)	183,111	0.0	2326	11.9
Organic N (kg $month^{-1}$)	1985–2010	2,947,230	–	270,050	–
	2025–2050 (CC + LU)	2 308 500	−21.7	224,272	−17
	2025–2050 (CC)	2,381,800	−19.2	205,189	−24.1
	2025–2050 (LU)	2,981,423	1.1	301,765	11.7
Organic P (kg $month^{-1}$)	1985–2010	753,573	–	94,087	–
	2025–2050 (CC + LU)	1,200,161	59.2	154,950	64.6
	2025–2050 (CC)	963,538	27.8	114,282	21.4
	2025–2050 (LU)	905,373	20.1	121,745	29.3
Mineral P (kg $month^{-1}$)	1985–2010	227,579	–	26,693	–
	2025–2050 (CC + LU)	523,044	129.8	60,436	126.4
	2025–2050 (CC)	346,803	52.3	39,818	49.1
	2025–2050 (LU)	330,409	45.1	39,380	47.5

CC = climate change; LU = land use change.

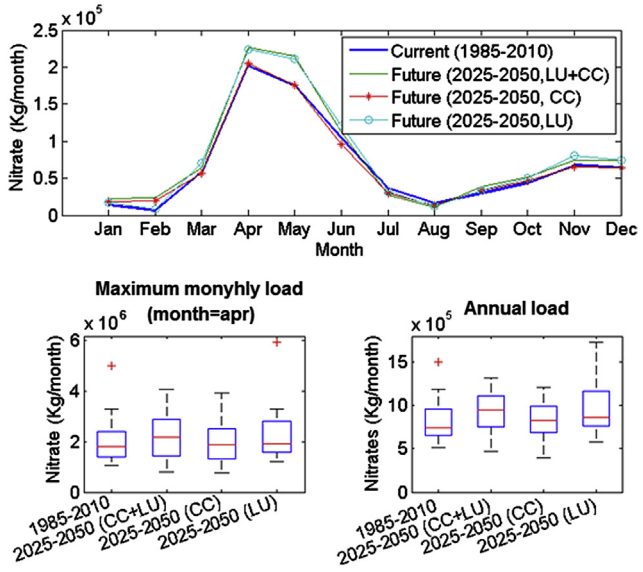

Fig. 9. Climate and land use changes impacts on Nitrate. Upper panel: average monthly nitrate load under current climate and land use (continuous blue line), under future land use and climate (continuous green line), under current land use and future climate (red line with star dots) and under future land use and current climate (cyan line with circular dots); Lower-left panel: boxplot of the maximum monthly load; Lower-right panel: boxplot of the annual load; CC: accounting for climate change; LU: accounting for land use changes. (For interpretation of the references to color in this figure legend, the reader is referred to the web version of this article.)

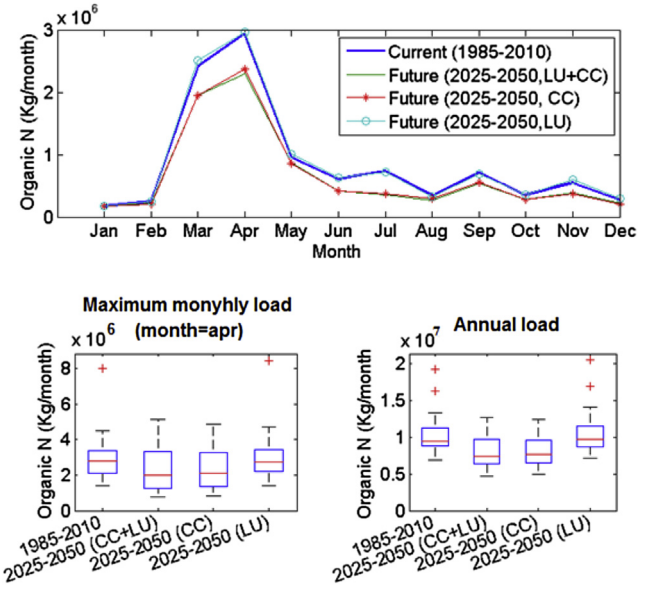

Fig. 11. Climate and land use changes impacts on Organic Nitrogen. Upper panel: average monthly organic N load under current climate and land use (continuous blue line), under future land use and climate (continuous green line), under current land use and future climate (red line with star dots) and under future land use and current climate (cyan line with circular dots); Lower-left panel: boxplot of the maximum monthly load; Lower-right panel: boxplot of the annual load; CC: accounting for climate change; LU: accounting for land use changes. (For interpretation of the references to color in this figure legend, the reader is referred to the web version of this article.)

experiment 1 (current conditions) and experiment 4 (current climate and projected land use) are almost similar (Fig. 8, upper panel); similarly, the average hydrograph of experiments 2 (projected climate and land use) is almost similar to the one of experiment 3 (projected climate, current land use), suggesting that land use changes will have very little influence on streamflow in the SN River basin. It can be seen in Table 4 for instance that climate change causes an 11.2% increase in mean flow and an 8.5% increase

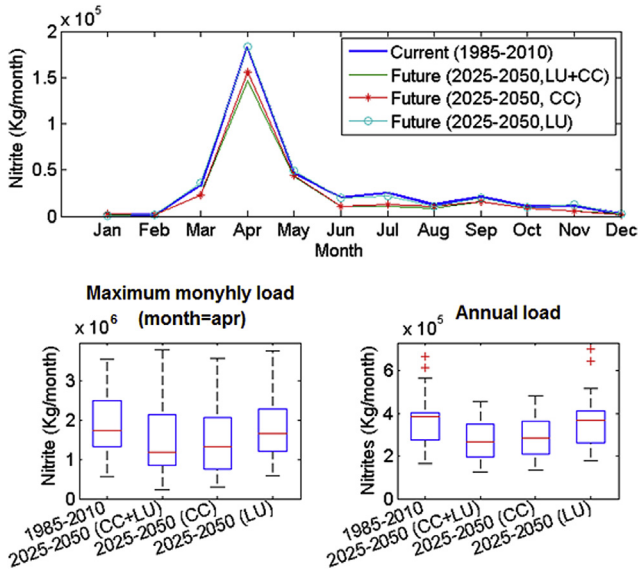

Fig. 10. Climate and land use changes impacts on nitrite. Upper panel: average nitrite N load under current climate and land use (continuous blue line), under future land use and climate (continuous green line), under current land use and future climate (red line with star dots) and under future land use and current climate (cyan line with circular dots); Lower-left panel: boxplot of the maximum monthly load; Lower-right panel: boxplot of the annual load; CC: accounting for climate change; LU: accounting for land use. (For interpretation of the references to color in this figure legend, the reader is referred to the web version of this article.)

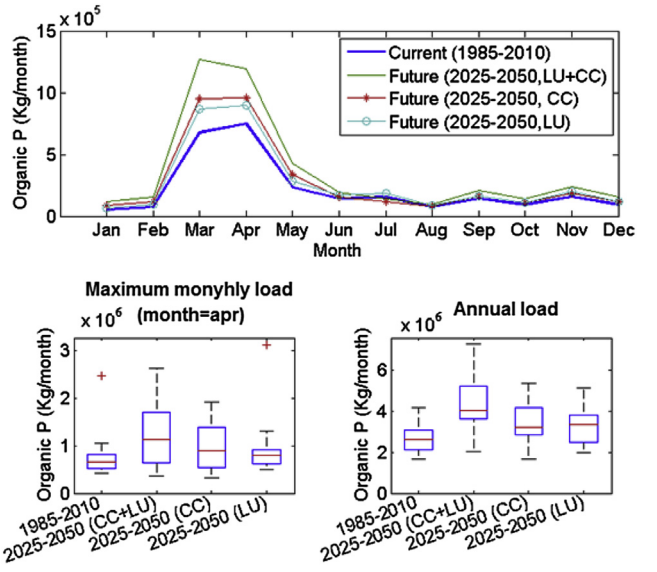

Fig. 12. Climate and land use changes impacts on Organic Phosphorus. Upper panel: average monthly organic P load under current climate and land use (continuous blue line), under future land use and climate (continuous green line), under current land use and future climate (red line with star dots) and under future land use and current climate (cyan line with circular dots); Lower-left panel: boxplot of the maximum monthly load; Lower-right panel: boxplot of the annual load; CC: accounting for climate change; LU: accounting for land use changes. (For interpretation of the references to color in this figure legend, the reader is referred to the web version of this article.)

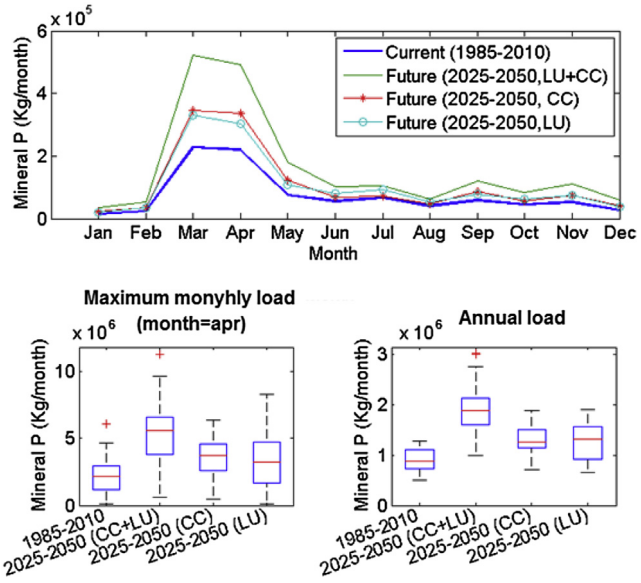

Fig. 13. Climate and land use changes impacts on Mineral Phosphorus. Upper panel: average monthly mineral P load under current climate and land use (continuous blue line), under future land use and climate (continuous green line), under current land use and future climate (red line with star dots) and under future land use and current climate (cyan line with circular dots); Lower-left panel: boxplot of the maximum monthly load; Lower-right panel: boxplot of the annual load; CC: accounting for climate change; LU: accounting for land use changes. (For interpretation of the references to color in this figure legend, the reader is referred to the web version of this article.)

in the maximum monthly flow; projected changes in land use alone would lead to only 2.6% and 1.2% increases of the maximum monthly flows and mean flow respectively. The combined effect of land use and climate change is not additive and leads to 11.0% and 12.3% increase in maximum monthly flows and mean flow respectively. These variations are however within the inter-annual variability of both maximum monthly flow (Fig. 8, lower left panel) and annual flow (Fig. 8, lower right panel). The magnitudes of the impacts on streamflow obtained in this study differ significantly from those of Tong et al. (2012) and Liu et al. (2000), where the impacts of land use changes are significant when compared to those of climate change, but are in line with what is projected in some parts of Scotland (Sample et al., 2012).

The impact of climate change on nitrate was found to be negligible since experiments 1 and 3 (and similarly experiments 2 and 4) load had almost the same average monthly nitrate load (Fig. 9, upper panel). Climate change alone leads to a 0.1% decrease in the annual nitrate load and a 1.4% increase of the maximum monthly nitrate load (Table 4). The same table shows that projected land use changes account for 10.6% increase of the maximum monthly nitrate load and a 14.0% increase of the annual nitrate load. The combined effect is an 11.7% increase of the maximum monthly load and 15.5% increase of the annual load. Climate change decreases nitrite loads at the annual scale (9.4%) while land use changes drive it up by 11.9% (Fig. 10, Table 4). The combined effect is an increase of 2.9%. A similar pattern can be observed for organic nitrogen (Fig. 11, Table 4), suggesting that land use changes will drive changes in nitrogen species in the SN River, as might be expected since nitrogen is a primary source of fertilizer for crops grown in this agriculturally dominated river basin. Tong et al. (2012) and Liu et al. (2000) found similar effects of climate change and land use change on nitrogen loading in Ohio Rivers that had agricultural influence. Both land use and climate change will lead to an increase in organic phosphorus (Fig. 12, Table 4) and mineral phosphorus (Fig. 13, Table 4) in the SN River. Their respective contributions are roughly equal, with climate change contributing marginally more than land use to the increase of the maximum monthly loads. At the annual time scale, land use change will lead to a slightly lower increase in mineral phosphorus load (+49.1%) relative to climate change (+47.5%).

The fact that the direction and magnitude of the calculated changes differ from those of other published studies is not surprising because each watershed/basin has unique features that contribute variable to sources of N and P. For instance, it was expected that streamflow would be sensitive to land use changes in mainly urbanized areas such as the ones described in Liu et al. (2008) and Felzer (2012). Given that the SN River basin will still be predominately rural by 2050, the fact that water quantities are projected to be less affected by land use changes is not surprising. Another watershed in the same region with a different urban to rural ratio, or a different land use change dynamic, will not necessarily have the same variations or even the same direction of change in water quality. Therefore, climate change and land use impact estimates should be conducted on a case-by-case basis. However, the methodology presented in this paper can be applied to any watershed in the world, in order to help more holistically define relative impacts of climate change and land use changes on water quantity and quality. Since it is easier and faster to adjust land use conversion trends than global warming trends, such studies may help guide land use authorities on how to zone and develop in the context of minimizing water pollution to downstream receptors. Knowledge of the direction and magnitude of the changes attributable to land use projection and climate change is of the greatest importance for the development of local water quality improvement policies or zoning restrictions and regulations. In the specific case of the SN River basin, the most durable solutions should target one or several of the following aspects: a) the rate of expansion of croplands; b) water management on croplands; c) areas of cropland development; and d) areas of urban development. An example of a potential adaptation strategy could be a restriction of fertilizer application on croplands that are too close to the water body (increasing fertilizer application set-backs or managing field drainage), and/or imposing land management practices that reduce runoff from farmland and urban areas. Once an adaptation measure targeting one of these aspects is defined, either the land use allocation model or the hydrological model could be run to estimate its added value in terms of water quality improvement potential.

It should be emphasized that the results presented here represent only one climate model (CRCM4.1.1) and one climate change scenario (A2). Repeating the experiments with other climate models and other climate change scenarios will help clarify how sensitive the results are, and provide a range for the expected changes in water quality and water quantity parameters for different climate input scenarios.

4. Conclusions

Six water quality and water quantity parameters were simulated using the SWAT model of the South Nation river basin in eastern Ontario Canada, using historical and projected 2025–2050 climate and land use projection data as hydrological model input. The future climate scenarios correspond to SRES scenario A2 which was obtained by correcting the outputs of the Canadian RCM with a combination of quantile–quantile transformation and nearest-neighbor search. Future land use maps were generated using a land use allocation model in the companion paper El-Khoury et al. (2014). Results show that climate change will be driving maximum monthly streamflow, nitrate, and organic phosphorus loads up,

while decreasing organic nitrogen and nitrite loads; land use changes will drive the same variables in the same direction as climate change, except for organic nitrogen, for which the effects of the two stressors are opposite. The magnitudes of the impacts are not the same and vary according to the water quality or quantity parameter: changes in streamflow will mainly be driven by climate change, whereas changes in nitrogen species will mainly be driven by land use changes. The contribution of climate change and land use changes on the increase of organic and mineral phosphorus are roughly equal. Furthermore, the effects of climate change and land use change cannot be considered linearly cumulative as the combined effects on water quality/quantity endpoints can be significantly different from the sum of the effect of each stressor/driver. The key finding in this study is that land use changes can have a significant impact on the future hydrological cycle of the South Nation River, and that failure to account for land use changes may lead to improper or inaccurate assessment of adaptation strategies that temper water pollution sources and drivers. From a global perspective, the study illustrates the importance of simultaneously accounting for climate and land use changes to estimate future changes in water quality and quantity variables.

References

Abbaspour, K.C., Vejdani, M., Haghighat, S., 2007. SWAT-CUP calibration and uncertainty programs for SWAT. In: Oxley, L., Kulasiri, D. (Eds.), Proc.Intl. Congress on Modelling and Simulation (MODSIM'07). Modelling and Simulation Society of Australia and New Zealand, Melbourne, Australia, pp. 1603–1609.

Arnold, J.G., Srinivasan, R., Muttiah, R.S., Williams, J.R., 1998. Large area hydrologic modelling and assessment part I; model development. J. Am. Water Resour. Assoc. 34, 73–89.

Barlage, M.J., Richards, P.L., Sousounis, P.J., Brenner, A.J., 2002. Impacts of climate change and land use change on runoff from a great lakes watershed. J. Gt. Lakes. Res. 28, 568–582.

Bingner, R.L., Theurer, F.D., Yuan, Y., 2007. AnnAGNPS Technical Processes. Available at: ftp://199.133.90.201/pub/outgoing/AGNPS/AGNPS_Web_Files/pdf_files/AnnAGNPS_Technical_Documentation.pdf (accessed 15.06.09.).

Burger, G., Murdock, T.Q., Werner, A.T., Sobie, S.R., Cannon, A.J., 2012. Downscaling extremes: an intercomparison of multiple statistical methods for present climate. J. Clim. 25, 4366–4388.

Burger, G., Sobie, S.R., Cannon, A.J., Werner, A.T., Murdock, T.Q., 2013. Downscaling extremes: an intercomparison of multiple methods for future climate. J. Clim. 26, 3429–3449.

CH2MHILL, 2001. Eastern Ontario Water Resources Management Study Final Report.CH2MHILL.

Chen, H., Xu, C.-Y., Guo, S., 2012. Comparison and evaluation of multiple GCMs, statistical downscaling and hydrological models in the study of climate change impacts on runoff. J. Hydrol. 434–435, 36–45.

Chiew, F., Kirono, D., Kent, D., Frost, A., Charles, S., Timbal, B., Nguyen, K., Fu, G., 2010. Comparison of runoff modelled using rainfall from different downscaling methods for historical and future climates. J. Hydrol. 387, 10–23.

Dibike, Y.B., Coulibaly, P., 2005. Hydrologic impact of climate change in the Saguenay watershed: comparison of downscaling methods and hydrologic models. J. Hydrol. 307, 145–163.

Dunn, S., Brown, I., Sample, J., Post, H., 2012. Relationships between climate, water resources, land use and diffuse pollution and the significance of uncertainty in climate change. J. Hydrol. 434–435, 19–35.

El-Khoury, A., Seidou, O., Lapen, D.R., Sunohara, M., Que, Z., Mohammadian, M., Bahram, D., 2014. Prediction of land-use conversions for use in watershed-scale hydrological modeling: a Canadian case study. Can. Geogr. http://dx.doi.org/10.1111/cag.1210 (published online 22/08/2014).

Environment Canada, 2008. Archived Hydrometric Data. Environment Canada. http://www.wsc.ec.gc.ca/applications/H2O/index-fra.cfm.

Felzer, B.S., 2012. Carbon, nitrogen, and water response to climate and land use changes in Pennsylvania during the 20th and 21st centuries. Ecol. Model. 240, 49–63.

Gachon, P., Radojevic, M., Pison, E., Saad, C., Lefaivre, L., 2009. DAI (Data Access Integration) Atlas: Climatological Maps from the Canadian RCM & the Canadian Global Climate Model Simulations over North America for the Current (1961–1990) & Future (2041–2070) Periods. Retrieved from:http://loki.qc.ec.gc.ca/DAI/doc/catalogue/DAI/s/do5(A)TLAS/s/do5(V)1.0/s/do5(F)EB26th2009.pdf.

Jakob Themeßl, M., Gobiet, A., Leuprecht, A., 2011. Empirical-statistical downscaling and error correction of daily precipitation from regional climate models. Int. J. Climatol. 31, 1530–1544.

Kalnay, E., Kanamitsu, M., Kistler, R., Collins, W., Deaven, D., Gandin, L., Iredell, M., Saha, S., White, G., Woollen, J., Zhu, Y., Leetmaa, A., Reynold, R., 1996. The NCEP/NCAR 40-Year reanalysis project. Bull. Amer. Meteor. Soc. 77, 437–471. http://dx.doi.org/10.1175/1520-0477(1996)077%3c0437:TNYRP%3e2.0.CO;2.

Kim, J., Choi, J., Choi, C., Park, S., 2013. Impacts of changes in climate and land use/land cover under IPCC RCP scenarios on streamflow in the Hoeya River basin. Korea. Sci. Total Environ. 452–453, 181–195.

Legesse, D., Vallet-Coulomb, C., Gasse, F., 2003. Hydrological response of a catchment to climate and land use changes in tropical Africa: case study south central Ethiopia. J. Hydrol. 275, 67–85.

Liu, A., Tong, S., Goodrich, J., 2000. Land use as a mitigation strategy for the water-quality impacts of global warming: a scenario analysis on two watersheds in the Ohio River basin. Environ. Eng. Policy 2, 65–76.

Liu, J., Zhang, L., Zhang, Y., Hong, H., Deng, H., 2008. Validation of an Agricultural Non-point Source (AGNPS) pollution model for a catchment in the Jiulong River watershed, China. J. Environ. Sci. 20, 599–606.

Maraun, D., Wetterhall, F., Ireson, A.M., Chandler, R.E., Kendon, E.J., Widmann, M., Brienen, S., Rust, H.W., Sauter, T., ThemeÃŸl, M., Venema, V.K.C., Chun, K.P., Goodess, C.M., Jones, R.G., Onof, C., Vrac, M., Thiele-Eich, I., 2010. Precipitation downscaling under climate change: recent developments to bridge the gap between dynamical models and the end user. Rev. Geophys. 48 http://dx.doi.org/10.1029/2009RG000314. http://doi.wiley.com/10.1029/2009RG000314.

Ministry of the Environment, 2009. Provincial (Stream) Water Quality Network. Ministry of the Environment, Government of Ontario, Toronto, Ontario. Accessible at: https://www.ontario.ca/environment-and-energy/provincial-stream-water-quality-monitoring-network-pwqmn-data.

Philips, S., Laanbroek, H.J., Verstraete, W., 2002. Origin, causes and effects of increased nitrite concentrations in aquatic environments. Rev. Environ. Sci. Biotechnol. 1, 115–141.

Que, Z., 2011. Evaluation of the Impact of Controlled Tile Drainage on Surface Water Quality in the South Nation River Watershed (Unpublished master thesis). University of Ottawa, Ottawa, Canada.

Reuter, H.I., Nelson, A., Jarvis, A., 2007. An evaluation of void filling interpolation methods for SRTM data. Int. J. Geogr. Inf. Sci. 21 (9), 983–1008.

Sala, O.E., 2000. Global biodiversity scenarios for the year 2100. Science 287, 1770–1774.

Sample, J., Dunn, S., Brown, I., Towers, W., 2012. Scotland's Water Resources: Impacts of Land Use and Climate.

Semenov, M.A., Barrow, E.M., 2002. LARS-WG: a stochastic weather generator for use in climate impact studies. Rothamsted Res.. Retrieved June 15, 2013 from: http://www.rothamsted.ac.uk/mas-models/download/LARSWG-Manual.pdf

Seung-Hwan, Y., Jin-Yong, C., Sang-Hyun, L., Yun-Gyeong, O., Dong Koun, Y., 2013. Climate change impacts on water storage requirements of an agricultural reservoir considering changes in land use and rice growing season in Korea. Agric. Water Manag. 117, 43–54.

Soil Landscapes of Canada Working Group, 2010. Soil Landscapes of Canada Version 3.2. (Digital Map and Database at 1:1 Million Scale). Agriculture and Agri-Food Canada, Ottawa, Ontario.

Tong, S.T., Sun, Y., Ranatunga, T., He, J., Yang, Y.J., 2012. Predicting plausible impacts of sets of climate and land use change scenarios on water resources. Appl. Geogr. 32, 477–489.

Tu, J., 2009. Combined impact of climate and land use changes on streamflow and water quality in Eastern Massachusetts, USA. J. Hydrol. 379, 268–283.

Wilby, R.L., Dawson, C.W., Barrow, E.M., 2002. SDSM – a decision support tool for the assessment of regional climate change impacts. Environ. Model. Softw. 17, 145–157.

Wilson, C.O., Weng, Q., 2011. Simulating the impacts of future land use and climate changes on surface water quality in the Des Plaines River watershed, Chicago metropolitan statistical area. Ill. Sci. Total Environ. 409, 4387–4405.